Pions in proton structure and everywhere else

Mary Alberg,[1,2,*] Lucas Ehinger,[1,†] and Gerald A. Miller[2,‡]
[1]*Department of Physics, Seattle University, Seattle, Washington 98122, USA*
[2]*Department of Physics, University of Washington, Seattle, Washington 98195, USA*

(Received 12 September 2021; accepted 21 June 2022; published 30 June 2022)

The pion cloud is important in nuclear physics and in a variety of low-energy hadronic phenomena. We argue that it is natural to expect it to also be important in lepton-proton deep inelastic scattering and Drell-Yan studies of proton structure. We compute the necessary consequences of the pion cloud in connection with the recent SeaQuest data. The effects are detailed by using the exact kinematics of the experiment. Good agreement with the measurements is obtained. Thus, the universality of pionic effects is understood.

DOI: 10.1103/PhysRevD.105.114054

The recent striking experimental finding [1] that antidown quarks are more abundant in the proton than antiup quarks for all observed values of the Bjorken x variable demands an interpretation and assessment of the consequences. This paper is aimed at providing such.

The results of [1] provide definitive experimental measurements of the ratio $\bar{d}/\bar{u}$. Although our early prediction [2] using a pion cloud model is in qualitative agreement with that experiment, it is necessary to update the calculation by providing results for the specific kinematics of the experiment that are known only since the publication [1].

We begin by explaining why it is natural to expect that the pion cloud would play a role in probes of proton structure. Pion exchange between nucleons provides in the one pion exchange potential (OPEP) the longest-ranged component of the strong force. It is an element of all models, from the ancient to the newest, of the nucleon-nucleon interaction. The OPEP is crucially responsible for the binding of nuclei [3,4]. Moreover, the presence of the pion as a significant component of the nuclear wave function is reinforced by the dominance of the pion in meson exchange corrections to a variety of nuclear properties. This was discussed long ago [5,6] and recently [7].

If a nucleon emits a virtual pion that is absorbed on another nucleon, as in the OPEP, it can emit a pion that is absorbed by itself. This is because nucleons are identical particles and a pion can be absorbed on any nucleon. Thus, the nucleon must consist, at least part of the time, of a nucleon and a virtual pion. The very significant contributions of pions to nucleon and baryon properties have been well documented for a long time [8–12]. Particular examples in which the pion-cloud effects are prominent are the neutron charge distribution [9] and baryon magnetic moments [11].

Given that the proton wave function has $n\pi^+(u\bar{d})$ and $p\pi^0$ components, with a two to one ratio of probabilities, there should be more antidown quarks than antiup quarks in the nucleon. This means that the textbook description that nucleons are composed of u and d valence constituent quarks, cannot be the whole story. Furthermore, the gluons inherent in QCD generate quark-antiquark pairs via perturbative interactions. Thus, one is led to the question; Do the pairs arise only from perturbative evolution at high momentum scales, or do they have a nonperturbative origin as in the pion cloud? A definitive answer would provide great help in understanding the nature of confinement and also the fundamental aspects of the nucleon-nucleon force. Perturbative QCD predicts a sea that is almost symmetric in light flavor. However, the discovery of the violation of the Gottfried sum rule told us that $\bar{d}$ quarks are favored over $\bar{u}$ quarks [13]. This highlighted the importance of the pion cloud of the nucleon [14,15]. Reviews are presented in [16–19]. More recent calculations of the difference $\bar{d}-\bar{u}$, the isovector component of the proton sea, have been published in [20–23]. We focus on the ratio $\bar{d}/\bar{u}$, determined by the SeaQuest experiment. The ratio has been a greater challenge for theory, since it depends on both the isoscalar and isovector components of the sea.

The concept of a component of a nucleon wave function makes sense only within a light front description of the nucleon. Our previous formalism [2] provided a light cone perturbation theory approach capable of making predictions with known uncertainties. Previous calculations had noted ambiguities related to the dependence of the pion-baryon vertex function on momentum transfer and on the possible dependence upon the square of the four-momentum of intermediate baryons, and much discussion ensued [16,24–34]. Another more fundamental issue involving the loss of relativistic invariance occurs when

*alberg@seattleu.edu
†ehingerlucas@seattleu.edu
‡miller@uw.edu

the vertex function is treated as depending on only three of the four necessary momentum variables. Our formalism resolved both of these problems by using a four-dimensional formalism and by using experimental constraints on the pion-baryon vertex function.

In a light-front formalism the proton wave function can be expressed as a sum of Fock-state components [35–38]. Our hypothesis is that the nonperturbative light-flavor sea originates from the bare nucleon, pion-nucleon (πN) and pion-Delta ($\pi\Delta$) components. The interactions are described by using the relativistic leading-order chiral Lagrangian [39,40]. Displaying the interaction terms to the relevant order in powers of the pion field, we use

$$\mathcal{L}_{\rm int} = -\frac{g_A}{2f_\pi}\bar{\psi}\gamma_\mu\gamma_5\tau^a\psi\partial_\mu\pi^a - \frac{1}{f_\pi^2}\bar{\psi}\gamma_\mu\tau^a\psi\epsilon^{abc}\pi^b\partial_\mu\pi^c - \frac{g_{\pi N\Delta}}{2M}(\bar{\Delta}^i_\mu g^{\mu\nu}\psi\partial_\nu\pi^i + \text{H.c.}), \quad (1)$$

where ψ is the Dirac field of the nucleon, π^a ($a = 1, 2, 3$) is the chiral pion field, and M is the nucleon mass. In Eq. (1) g_A denotes the nucleon axial-vector coupling and f_π the pion-decay constant. The second term is the Weinberg-Tomazowa term which describes low-energy π-nucleon scattering. In the third term $g_{\pi N\Delta}$ is the $\pi N\Delta$ coupling constant, and the Δ^i_μ field is a vector in both spin and isospin space.

The light-front Hamiltonian operator is constructed from the T^{+-} component of the energy momentum tensor [35,36,38,41,42]. The Hamiltonian can be written in terms of a sum of kinetic energy operators, M_0^2 and interaction terms, denoted as V, see Fig. 1. The first two terms are standard interactions, and the third is an instantaneous term that enters only at higher orders in the coupling constant. The Hamiltonian forms of the single-pion emission or absorption terms (Fig. 1) are expressed as matrix elements evaluated between on-shell free nucleon spinors. The light-front Schrödinger equation for the proton, p, is given by $(M_0^2 + V)|p\rangle = M_p^2|p\rangle$. To the desired second order it is

$$|p\rangle \approx \sqrt{Z}|p\rangle_0 + \frac{1}{M_p^2 - M_0^2}V|p\rangle_0, \quad (2)$$

where $|p\rangle_0$ represents the nucleon in the absence of the pion cloud, the bare nucleon, and Z is a normalization constant. Given Eq. (2), the wave function can be expressed as a sum of Fock-space components given by

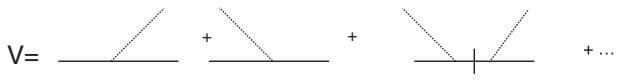

FIG. 1. Terms in the light-front Hamiltonian.

$$|p\rangle = \sqrt{Z}|p\rangle_0 + \sum_{B=N,\Delta}\int d\Omega_{\pi B}|\pi B\rangle\langle\pi B|p\rangle_0, \quad (3)$$

where $\int d\Omega_{\pi B}$ is a phase-space integral [37,38]. In this formalism the pion momentum distributions $f_{\pi B}(y)$, which represent the probability that a nucleon will fluctuate into a pion of light front momentum fraction y and a baryon of light front momentum fraction $1 - y$, are squares of wave functions, $|\langle\pi B|\Psi\rangle|^2$ integrated over $k_\perp$.

The Lagrangian of Eq. (1) is incomplete because it is not renormalizable. We tame divergences using a physically motivated set of regulators, depending on four-momenta, that are constrained by data. If chiral symmetry is maintained, one finds that the πN vertex function $g_{\pi N}(t)$ and the nucleon-axial form factor are related by the generalized Goldberger-Treiman relation [43] (obtained with $m_\pi = 0$),

$$Mg_A(t) = f_\pi g_{\pi N}(t), \quad (4)$$

$$g_A(t) = g_A(0)/(1 + (t/M_A^2))^2, \quad (5)$$

where t is the square of the four-momentum transferred to the nucleon. Equation (4) follows from partial conservation of the axial-vector current (PCAC) and the pion pole dominance of the pseudoscalar current. It is obtained from a matrix element of the axial vector current between two on-mass shell nucleons. The t dependence of g_A is determined for $t > 0$ by low-momentum transfer experiments [43], with M_A being the single parameter. Equation (4) relates an essentially unmeasurable quantity $g_{\pi N}(t)$ with one $g_A(t)$ that is constrained by experiments. The major uncertainty in previous calculations is largely removed. Some models, see e.g., [44], find differences between the t dependence of $g_A(t)$ and $g_{\pi N}(t)$, which is allowed because $m_\pi \neq 0$. Uncertainties in the parameter M_A are discussed in [2], where it is also shown that very large values of t are not important in the calculations of this paper.

In evaluating the nucleon wave function Eq. (3) the necessary vertex function must be applicable to situations when either the pion or the baryon or both are off their mass shells. We use frame-independent pion-baryon form factors, in which a nucleon of mass M and momentum p emits a pion of mass μ and momentum k and becomes a baryon of mass M_B and momentum $p - k$,

$$F(k,p,y) = \frac{\Lambda^2}{k^2 - \mu^2 - \Lambda^2 + i\epsilon}\frac{\Lambda^2}{\frac{y}{1-y}((p-k)^2 - M_B^2) - \Lambda^2 + i\epsilon}, \quad (6)$$

where $y = k^+/p^+$.

Using $F(k,p,y)$ allows us to obtain a pion-baryon light front wave function. The pion-nucleon component is given by

$$\Psi_{\mathrm{a,LF}}(k,p,s)=\frac{Mg_A}{2f_\pi(2\pi)^{3/2}}\sqrt{\frac{y}{1-y}}\frac{\bar{u}(p-k)i\gamma^5\tau_a u(p)}{t+\mu^2}F_A(t),$$
$$F_A(t)\equiv\frac{2\Lambda^4}{(\Lambda^2+t+\mu^2)(2\Lambda^2+t+\mu^2)}, \tag{7}$$

with s and a the spin and isospin labels for the proton. Expanding $F_A(t)$ to first order in t, then comparing the result to the same expansion of $g_A(t)/g_A(0)$ and matching the results determines the value $\Lambda=\sqrt{3}/2M_A$. Using this, $F(k,p,y)$ is equivalent to using a form factor of the form of Eq. (4) in computing $f_{\pi N}(y)$ [2]. The parameter-independence of this approach is maintained.

The pion 2D-momentum distribution function $f_{\pi N}(y,t)$ is obtained by squaring $|\Psi_{\mathrm{a,LF}}(k,p,s)|$ and summing over a, s. The result is

$$f_{\pi N}(y,t)=\frac{3M^2}{16\pi^2}\frac{g_A^2}{f_\pi^2}y\frac{t}{(t+\mu^2)^2}F_A^2(t), \tag{8}$$

with $t=(M^2y^2+k_\perp^2)/(1-y)$. The pion longitudinal-momentum distribution function $f_{\pi N}(y)$ is then

$$f_{\pi N}(y)=\int_{t_N}^{\infty}dt f_{\pi N}(y,t), \tag{9}$$

where $t_N\equiv M^2y^2/(1-y)$. Using Eq. (4) or Eq. (7) yields the same $f_{\pi N}$ because the integrand is dominated by the region of low values of t. The pionic effects were shown to be of long range [2] by studying the resulting three-dimensional light front structure of the pion-baryon wave function.

The intermediate Δ contribution is important because it is sizable and tends to favor $\bar{u}$ over $\bar{d}$. We found [2] that

$$f_{\pi\Delta}(y)=\frac{1}{12\pi^2}\left(\frac{g_{\pi N\Delta}}{2M}\right)^2 y\int_{t_\Delta}^{\infty}dt\frac{F_A^2(t)}{(t+\mu^2)^2}$$
$$\times\left(t+\frac{1}{4M_\Delta^2}(M^2-M_\Delta^2+t)^2\right)((M+M_\Delta)^2+t), \tag{10}$$

with $t_\Delta=(y^2M^2+y(M_\Delta^2-M^2))/(1-y)$.

Next we use the Fock-space wave function of Eq. (3) to compute the light-flavor sea component of the nucleon wave function. Consider the role of the pion cloud in deep inelastic scattering (DIS) (see Fig. 2). One needs to include terms in which the virtual photon hits: (a) the bare nucleon, (b) the intermediate pion [45], and (c) the intermediate baryon B of the (πB) Fock-state component. The key assumption of the present model is that quantum interference effects involving different Fock-space components are negligible because the different final states obtained from deep inelastic scattering by the pion and by the nucleon are expected to be orthogonal.

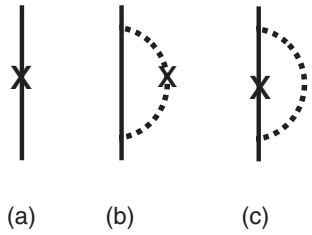

FIG. 2. (a) External interaction, X, with bare nucleon (solid line), (b) External interaction, X, with the pion, (c) External interaction, X, with the intermediate baryon. Here X represents the deep inelastic scattering operator.

The effects of the Weinberg-Tomazowa (WT) term vanish because the deep inelastic scattering operator, represented by X in the figure is diagonal in the pion-flavor index [2].

Given the lack of interference effects, one can represent at any Q^2 the quark distribution functions of flavor $f=(\bar{u},\bar{d})$ in the nucleon sea as

$$q_N^f(x,Q^2)=Zq_{N0}^f(x,Q^2)+\sum_B f_{\pi B}\otimes q_\pi^f+\sum_B f_{B\pi}\otimes q_B^f, \tag{11}$$

in which $B=N,\Delta$, and $f_{\pi B}\otimes q_\pi^f\equiv\int_x^1\frac{dy}{y}f_{\pi B}(y)q_\pi^f(\frac{x}{y},Q^2)$. The first symbol in the subscript represents the struck hadron, and the phase-space factor in Eq. (3) ensures that $f_{\pi B}(y)=f_{B\pi}(1-y)$, so that momentum is conserved. The quark distributions of the hadrons in the cloud are given by $q_\pi^f(x,Q^2)$ and $q_B^f(x,Q^2)$, and the bare nucleon distributions are given by $q_{N0}^f(x,Q^2)$. The model is defined by the Fock-state expansion [Eq. (3)] using meson-baryon states. The functions $f_{\pi B}(y)$ give the probability that the proton fluctuates into a pion-baryon component as a function of the pion-momentum fraction y. This defines the non-perturbative proton wave function that depends on the pion-baryon relative momentum and is necessarily independent of the momentum of any probe. This wave function is to be used to compute observables measured in reactions in which the probe interacts with the *hadrons* in the Fock-state expansion of the proton. Pionic components make their presence known in a variety of processes such as the computation of charge densities, magnetic moments, and the nucleon-nucleon interaction.

Next comes the issue of computing the structure functions obtained in deep inelastic scattering and in the Drell-Yan process. This involves the photon-quark interaction. At the high momentum transfers relevant for those processes, the photon interacts with the quarks, not with the hadrons.

The quark-structure functions $q(x)$ are given in terms of the number of quarks in the hadron wave function at $q(\xi)$ and a function C that incorporates the dynamics of the photon-quark interaction, in the schematic formula $q(x,Q^2) = \int d\xi q(\xi) C(x/\xi, Q^2)$ [46]. The function C can be regarded as an effective photon-quark cross section [47]. Thus the content of the model is that the evolution of the proton is contained in the evolution of the quarks that exist within the component hadrons.

Evolution of the quark parton distribution functions (pdfs) decreases the momentum fraction of the valence quarks as the momentum fractions of the sea quarks and gluons increase, but the momentum sum of all partons is still one.

We assume that pionic fluctuations are the only source of the flavor asymmetry of the proton sea. This is because all quark-gluon processes are flavor independent if the quarks have the same mass. We have dominant u, $\bar{u}$ and d, $\bar{d}$ quarks that are essentially massless. The bare proton and the intermediate Δ and nucleon pdfs have no contribution from pionic fluctuations, so they are flavor symmetric and we set $q^f_{N0} = q^f_\Delta = q^f_B$. We have suppressed the Q^2 dependence of q^f, q_{N0}, q^f_π, and q^f_B to simplify the notation.

Contributions to the antiquark sea of the proton come from the valence and sea distributions of the pion q^v_π and q^s_π and the sea distributions q^s_B and q^s_N of the intermediate baryons and the bare proton. The use of these distributions to describe deep inelastic scattering from a bound pion follows from the light front Fock-space expansion, Eq. (3), which involves only on-mass-shell constituents. With $f_{\pi^+ n} = \frac{2}{3} f_{\pi N}$, $f_{\pi^0 p} = \frac{1}{3} f_{\pi N}$, $f_{\pi^- \Delta^{++}} = \frac{1}{2} f_{\pi\Delta}$, $f_{\pi^0 \Delta^+} = \frac{1}{3} f_{\pi\Delta}$, $f_{\pi^+ \Delta^0} = \frac{1}{6} f_{\pi\Delta}$, the antiquark distributions are

$$\bar{d}(x) = \left(\frac{5}{6} f_{\pi N} + \frac{1}{3} f_{\pi\Delta}\right) \otimes q^v_\pi + \bar{q}_{\rm sym}(x), \quad (12)$$

$$\bar{u}(x) = \left(\frac{1}{6} f_{\pi N} + \frac{2}{3} f_{\pi\Delta}\right) \otimes q^v_\pi + \bar{q}_{\rm sym}(x), \quad (13)$$

where $\bar{q}_{\rm sym}(x) \equiv \sum_B f_{\pi B} \otimes q^s_\pi + \sum_B f_{B\pi} \otimes q^s_B + Z q^s_N(x)$. The πN terms favor the $\bar{d}$, but the $\pi\Delta$ terms favor the $\bar{u}$.

For comparison with SeaQuest results, Eqs. (11)–(13) require pion and baryon pdfs, $q^f_\pi(x,Q^2)$, $q^f_B(x,Q^2)$, and $q^f_{N0}(x,Q^2)$, at the scale of the SeaQuest experiment, $Q^2 = 25.5$ GeV^2. We use pdfs determined by different groups from their fits to experimental data. We evolve these pdfs to the SeaQuest scale before using them in Eqs. (12) and (13). This approach has been used in meson-cloud models for many decades. e.g., [24,25,32]. We describe our evolution procedures below.

Two pion parton distributions were used; those of Aicher, Schäfer, and Vogelsang (ASV) [48], and the more recent pion pdfs of the xFitter Collaboration [49], which are consistent with the pion pdfs of the JAM Collaboration [23], which have challenged the high-x behavior of the ASV valence pdfs. We evolved the ASV pion valence pdfs at next-to-leading order (NLO) from their starting scale of $Q^2_0 = 0.40$ GeV^2 to $Q^2 = 25.5$ GeV^2; the scale relevant for SeaQuest. Our fit to the evolved valence distribution is given by $q^v_\pi(x) = 1.38 x^{-0.320}(1-x)^{3.02}(7.40x^2+1)$. The ASV analysis used the pion sea-quark pdfs of Gluck, Reya, and Schienbein [50] at their starting scale. After NLO evolution to 25.5 GeV^2, $q^s_\pi(x) = 0.113 x^{-1.19}(1-x)^{5.10} \times (1 - 2.31\sqrt{x} + 4.08x)$. We used the xFitter pdf parametrization from the LHAPDF6 Library with ApfelWeb [51,52] to evolve their pdfs at NLO to the SeaQuest scale.

Holtmann *et al.* [24] explained that the bare-proton sea cannot be determined directly from experimental data, which includes contributions from the pion cloud. Their model for bare-proton parton distributions [53] used a fit to DIS data that included corrections to remove contributions from the pion cloud. In our updated calculation we used the program QCDNUM [54] to evolve, at NLO, their bare proton pdfs (valence, gluon, and sea) from the starting scale of $Q^2_0 = 4$ GeV^2 to the SeaQuest scale of $Q^2 = 25.5$ GeV^2. This is the only change to our previous calculation of the bare sea. We used the resulting bare-sea distribution for the contributions of the proton in Fig. 2(a) and the intermediate baryons of Fig. 2(c).

Other input parameters must be described before presenting numerical results. The pion-nucleon splitting function $f_{\pi N}(y)$ depends on the coupling constant $g_{\pi N}$ and the form factor cutoff Λ. The lower limit for $g_{\pi N}$ is 12.8, taken from the Goldberger-Treiman relation $g_{\pi N} = \frac{M}{f_\pi} g_A$, with $g_A = 1.267 \pm 0.04$, $M = 0.939$ GeV, and $f_\pi = 92.6$ MeV. The upper limit is $g_{\pi N} = 13.2$, consistent with the scattering data analysis of Perez *et al.* [55] and the muon-based determination of g_A by Hill *et al.* [56]. As noted above the cutoff parameter of Eq. (7), $\Lambda = \sqrt{3}/2M_A$ is obtained at very low t. The two resulting splitting functions are identical for all values of y, demonstrating that only small values of t are important in the present calculations. In the initial calculations we used the value $M_A = 1.03 \pm 0.04$ GeV [43]. This early review result was confirmed by many authors [57–61], all obtaining results within the stated uncertainty. We have increased the uncertainty in our cutoff Λ to $\pm 10\%$ to allow for a difference between the cutoffs in the πNN form factor and the axial form factor. Although one early estimate, based on the cloudy bag model, suggested that the difference might be $\pm 20\%$ [44], later work using dispersion relations found consistency between the axial form factor cutoff and a πNN *monopole* cutoff of $\Lambda = 0.80$ GeV $\pm$ 10% [62,63]. A monopole value of $\Lambda = 0.8$ GeV corresponds to a dipole value of 1.1 GeV.

The splitting function $f_{\pi N}(y)$ for a range of parameters bounded by the maximum and minimum values of $g_{\pi N}$ and Λ is shown in Fig. 3.

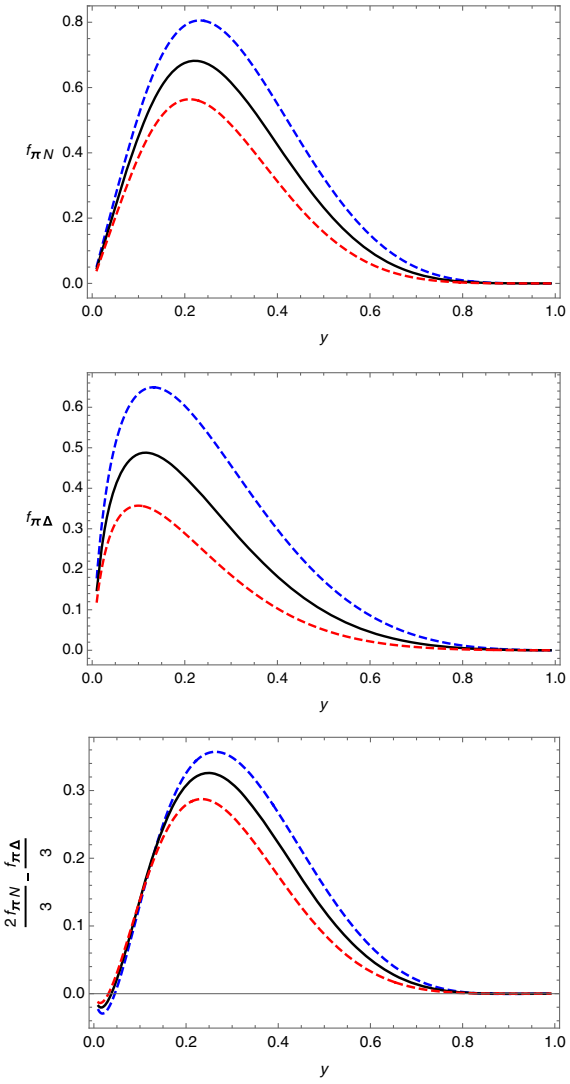

FIG. 3. Pion-baryon splitting functions $f_{\pi B}(y)$, $B = N, \Delta$, are shown in the upper two panels. The solid lines are found using the central values of our coupling constants and cutoffs. The upper (blue) and lower (red) dashed lines are obtained using the maximum or minimum values, respectively, of these parameters. The lowest panel shows the contribution of the splitting functions to the integrated asymmetry, $\bar{D} - \bar{U}$, Eq. (14). The smaller spread between the dashed lines is due to the correlation between the coupling constants and the use of the same cutoff in $f_{\pi N}(y)$ and $f_{\pi\Delta}(y)$.

The value of the $\pi N\Delta$ coupling constant plays an important role in our calculations. Both the upper limit $(\frac{g_{\pi\Delta}}{g_{\pi N}})^2 = \frac{72}{25}$, $g_{\pi\Delta} = 1.7 g_{\pi N}$ and the lower limit, obtained from the large N_C limit of $g_{\pi\Delta} = 1.5 g_{\pi N}$, are much smaller than the value $g_{\pi\Delta} = 2.2 g_{\pi N}$ extracted from the K-matrix analysis of [64]. This difference is important because the contribution of the intermediate Δ is proportional to $g^2_{\pi\Delta}$. The K-matrix analysis obtained $g_{\pi\Delta}$ from the width of the Δ computed for the dominant s-channel diagram. This analysis is incomplete because it neglects the influence of the iteration of the crossed pion-nucleon Born term that makes a substantial contribution to the width. The importance of that diagram was explained in the textbook [65]. A detailed calculation of the pion-nucleon scattering in the (3,3) channel was made in [8], which found a good description of the phase shift using quark-model values of the coupling constant. That work used a static approximation, but Niskanen [66] included higher-order effects which showed that the quark-model values of the coupling constants can be consistent with the experimental width. The definitive coupling-constant compilation [67] found values consistent with the large N_C limit. All of this early work was confirmed by recent calculations [68–70] that find values of $g_{\pi\Delta}$ in accord (within errors) of the large N_c calculations. Such values are consistent with the value extracted from the covariant Δ width at full one-loop order [69] and with the extraction from NN scattering [70]. Moreover, our range of values of $g_{\pi\Delta}$ are used routinely in calculations of the nucleon-nucleon potential [71]. The net result is that the range of values of $g_{\pi\Delta}$ that we use is consistent with the width of the Δ.

The splitting function $f_{\pi\Delta}(y)$ depends on the coupling constant $g_{\pi\Delta}$ and the form factor cutoff Λ. We use the same form factor and cutoff for $f_{\pi N}(y)$ and $f_{\pi\Delta}(y)$. The ratio $f_{\pi\Delta}(y)/f_{\pi N}(y)$ is less than unity for the important regions of y. It does increase as y increases above 0.5, and becomes greater than unity at about $y = 0.8$, where both splitting functions are vanishingly small. Reference [2], showed in a detailed discussion that the splitting functions arise from the long-range structure of the nucleon.

Finally, it has been known for a long time that the use of soft form factors (similar in range to those of the present study) leads to a convergent perturbation series [8–10,72] in the pion-baryon coupling constants. Having justified the model, let us turn to the observations. The integrated asymmetry $\bar{D} - \bar{U}$ is the difference in number of $\bar{d}$ and $\bar{u}$ quarks in the proton sea. With $\bar{D} = \int_0^1 \bar{d}(x)dx$, $\bar{U} = \int_0^1 \bar{u}(x)dx$, the asymmetry is determined from Eq. (12) and Eq. (13) as

$$\bar{D} - \bar{U} = \frac{2}{3}\int_0^1 dy f_{\pi N}(y) - \frac{1}{3}\int_0^1 dy f_{\pi\Delta}(y). \quad (14)$$

The experiment E866 [73] measured $\bar{D} - \bar{U} = 0.118 \pm 0.012$. Our splitting functions predict $0.098 \leq \bar{D} - \bar{U} \leq 0.131$, in excellent agreement with the experimental result. The computed values of $\bar{d}(x) - \bar{u}(x)$ are compared to the E866 results in Fig. 4, with bands obtained using minimum and maximum values of the splitting functions shown in Fig. 3, in convolution with ASV or xFitter pion pdfs. The band includes the sum of the two contributions; $p \to \pi N$ and $p \to \pi\Delta$. The width of the band is narrow because of the correlation between the coupling constants, $g_{\pi\Delta} = r g_{\pi N}$ with $1.5 \leq r \leq 1.7$, and the use of the same cutoff Λ for both terms. This band is a definitive prediction of the

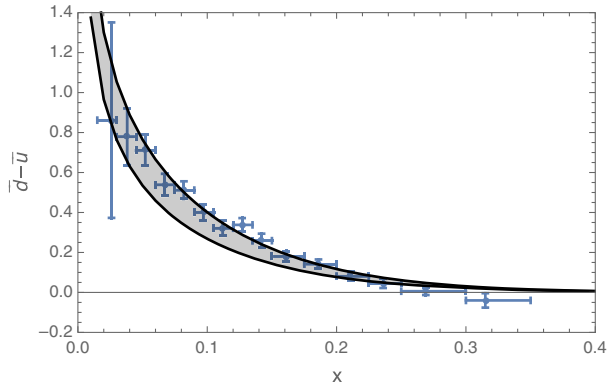

FIG. 4. $\bar{d}(x) - \bar{u}(x)$. Blue symbols from E866 [73]. The bands are computed using minimum and maximum values of the splitting functions shown in Fig. 3 in convolution with ASV or xFitter pion pdfs.

present model. We stress that in *any* model, $\bar{u}$ and $\bar{d}$ are correlated so that errors in each are partially cancelled in the ratio. We find that a 15% uncertainty in $\bar{d}$, $\bar{u}$, at $x = 0.3$ translates to 7% in the ratio.

Calculations of the ratio $\bar{d}(x)/\bar{u}(x)$ are compared with experimental data in Fig. 5. The results for values of x less than about 0.15 arise from a combination of pion-cloud effects and the symmetric sea of the bare nucleon. For larger values of x, terms of Fig. 2(b) dominate, with the πN contribution rising with increasing x until $x \approx 0.34$. The ratio then drops because of the enhancement of $\bar{u}$ [Eq. (13)] provided by the $\pi\Delta$ contribution, which becomes relatively more important as x increases.

Good agreement with experimental data is obtained for $x < 0.2$, but the decrease in the ratio $\bar{d}(x)/\bar{u}(x)$ found by E866 for higher values of x is not reproduced.

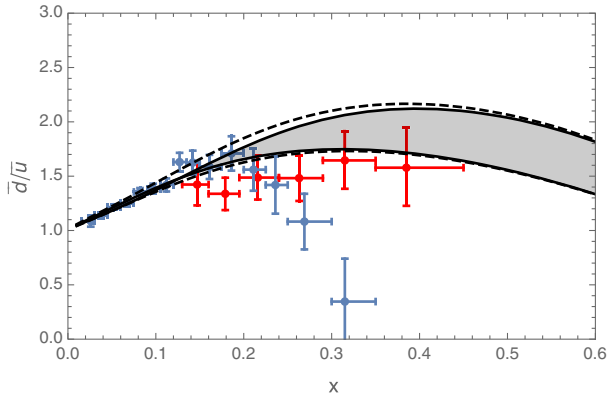

FIG. 5. $\bar{d}(x)/\bar{u}(x)$ Blue symbols from E866 [73]. Red symbols are from SeaQuest [1]. The solid band is computed using minimum and maximum values of the splitting functions shown in Fig. 3 in convolution with ASV or xFitter pion pdfs, plus the bare sea of [53]. All pdfs were evolved to the SeaQuest scale of $Q^2 = 25.5$ GeV^2. The dashed lines include the effects of varying the bare sea by a factor of 0.75 or 1.25.

Our calculations are in agreement with the new results of SeaQuest, which show a slight rise in the ratio $\bar{d}(x)/\bar{u}(x)$ in the x domain covered by the experiment, with a slight hint of a downturn as $x \to 0.4$. Our calculation predicts that this would signal the increasing influence of the $\pi\Delta$ contribution. The prediction of Kofler and Pasquini for $\bar{d}/\bar{u}$ [20] lies well above ours because it does not include the $\pi\Delta$.

The present results for the ratio $\bar{d}/\bar{u}$ are a bit smaller than those of our earlier calculation [2], but have a wider uncertainty band because we considered two pion pdfs. The lower ratio is caused by several factors, each of which increases $\bar{d}$ and $\bar{u}$. The dominant contribution to the proton sea comes from the valence antiquark distribution of the pion. The number of valence antiquarks is constant, but evolution increases $q_\pi^v(x)$ for $x < 0.2$ and decreases it for $x > 0.2$. In the latter domain, our evolution to the SeaQuest $Q^2 = 25.5$ GeV^2 yields higher $q_\pi^v(x)$ than our earlier evolution to the E866 $Q^2 = 54$ GeV^2, increasing the contributions of the first terms of Eqs. (12)–(13). The second terms of these equations make equal contributions to $\bar{d}$ and $\bar{u}$ from the symmetric sea quark pdfs of the pion and of the bare baryons. Evolution increases the total number of sea quarks. After convolution, the pion sea makes a small contribution to the proton sea, and its evolution has a small effect. In our earlier work we did not evolve the bare sea, so both $\bar{d}$ and $\bar{u}$ are increased in our present work. These increases in both numerator and denominator decrease the $\bar{d}/\bar{u}$ ratio, and bend our prediction band lower, improving its agreement with experiment.

Our 2019 paper said "The pion-baryon form factors of our model are essentially model independent, and the coupling constants are reasonably well determined. For values of x greater than about 0.15, the pion cloud effects dominate. The rise and then fall of the ratio $\bar{d}/\bar{u}$ are unalterable consequences of our approach. Significantly changing any of the input parameters would cause severe disagreements with other areas of nuclear physics, and would be tantamount to changing the model. If the high-x E866 results were to be confirmed by the SeaQuest experiment, the model would be ruled out".

It turned out that our predictions were in agreement with the SeaQuest data, even though we did not know the exact values of the kinematics. The present paper updates the earlier calculation by including evolution of the bare nucleon sea and using the now known SeaQuest kinematics. The present calculations show that the changes produce small effects, and further that our earlier prediction is improved to a good reproduction of the data.

The formalism presented here shows how to properly obtain pion-baryon vertex functions in a four-dimensional treatment that includes the effects of the uncertainties in the input parameters in a controlled fashion. Our result is a chiral light front perturbation theory calculation of the wave function that successfully describes the flavor content of the nucleonic light-quark sea.

This shows that pionic effects are here, there, and everywhere.

The work of M. A. and L. E. was supported by the Research in Undergraduate Institutions Program of the US National Science Foundation under Grant No. 2012982. The work of G. A. M. was supported by the USDOE Office of Science, Office of Nuclear Physics under Grant No. DE-FG02-97ER41014.

[1] J. Dove *et al.* (SeaQuest Collaboration), The asymmetry of antimatter in the proton, Nature (London) **590**, 561 (2021).
[2] Mary Alberg and Gerald A. Miller, Chiral light front perturbation theory and the flavor dependence of the light-quark nucleon sea, Phys. Rev. C **100**, 035205 (2019).
[3] Norbert Kaiser, R. Brockmann, and W. Weise, Peripheral nucleon-nucleon phase shifts and chiral symmetry, Nucl. Phys. **A625**, 758 (1997).
[4] Norbert Kaiser, S. Fritsch, and W. Weise, Chiral dynamics and nuclear matter, Nucl. Phys. **A697**, 255 (2002).
[5] D. O. Riska and G. E. Brown, Tensor force and exchange currents in the triton beta decay, Phys. Lett. **32B**, 662 (1970).
[6] D. O. Riska and G. E. Brown, Meson exchange effects in n + p− > d + gamma, Phys. Lett. **38B**, 193 (1972).
[7] G. B. King, L. Andreoli, S. Pastore, M. Piarulli, R. Schiavilla, R. B. Wiringa, J. Carlson, and S. Gandolfi, Chiral effective field theory calculations of weak transitions in light nuclei, Phys. Rev. C **102**, 025501 (2020).
[8] S. Theberge, Anthony William Thomas, and Gerald A. Miller, The cloudy bag model. 1. The (3,3) resonance, Phys. Rev. D **22**, 2838 (1980); **23**, 2106(E) (1981).
[9] Anthony William Thomas, S. Theberge, and Gerald A. Miller, The cloudy bag model of the nucleon, Phys. Rev. D **24**, 216 (1981).
[10] Serge Theberge, Gerald A. Miller, and Anthony William Thomas, The cloudy bag model. 4. Higher order corrections to the nucleon properties, Can. J. Phys. **60**, 59 (1982).
[11] S. Theberge and Anthony William Thomas, Magnetic moments of the nucleon octet calculated in the cloudy bag model, Nucl. Phys. **A393**, 252 (1983).
[12] V. Bernard, Norbert Kaiser, and Ulf-G. Meissner, Chiral dynamics in nucleons and nuclei, Int. J. Mod. Phys. E **04**, 193 (1995).
[13] P. Amaudruz *et al.* (New Muon Collaboration), The Gottfried Sum from the Ratio F2(n)/F2(p), Phys. Rev. Lett. **66**, 2712 (1991).
[14] Anthony William Thomas, A limit on the pionic component of the nucleon through SU(3) flavor breaking in the sea, Phys. Lett. **126B**, 97 (1983).
[15] E. M. Henley and G. A. Miller, Excess of anti-D over anti-U in the proton sea quark distribution, Phys. Lett. B **251**, 453 (1990).
[16] J. Speth and Anthony William Thomas, Mesonic contributions to the spin and flavor structure of the nucleon, Adv. Nucl. Phys. **24**, 83 (1997).
[17] Gerald T. Garvey and Jen-Chieh Peng, Flavor asymmetry of light quarks in the nucleon sea, Prog. Part. Nucl. Phys. **47**, 203 (2001).
[18] Wen-Chen Chang and Jen-Chieh Peng, Flavor structure of the nucleon sea, Prog. Part. Nucl. Phys. **79**, 95 (2014).
[19] D. F. Geesaman and P. E. Reimer, The sea of quarks and antiquarks in the nucleon, Rep. Prog. Phys. **82**, 046301 (2019).
[20] Stefan Kofler and B. Pasquini, Collinear parton distributions and the structure of the nucleon sea in a light-front meson-cloud model, Phys. Rev. D **95**, 094015 (2017).
[21] C. Cocuzza, W. Melnitchouk, A. Metz, and N. Sato (Jefferson Lab Angular Momentum (JAM) Collaboration), Bayesian Monte Carlo extraction of the sea asymmetry with SeaQuest and STAR data, Phys. Rev. D **104**, 074031 (2021).
[22] J. R. McKenney, Nobuo Sato, W. Melnitchouk, and Chueng-Ryong Ji, Pion structure function from leading neutron electroproduction and SU(2) flavor asymmetry, Phys. Rev. D **93**, 054011 (2016).
[23] P. C. Barry, N. Sato, W. Melnitchouk, and Chueng-Ryong Ji, First Monte Carlo Global QCD Analysis of Pion Parton Distributions, Phys. Rev. Lett. **121**, 152001 (2018).
[24] H. Holtmann, A. Szczurek, and J. Speth, Flavor and spin of the proton and the meson cloud, Nucl. Phys. **A596**, 631 (1996).
[25] W. Koepf, L. L. Frankfurt, and M. Strikman, The Nucleon's virtual meson cloud and deep inelastic lepton scattering, Phys. Rev. D **53**, 2586 (1996).
[26] M. Strikman and C. Weiss, Chiral dynamics and partonic structure at large transverse distances, Phys. Rev. D **80**, 114029 (2009).
[27] M. Strikman and C. Weiss, Quantifying the nucleon's pion cloud with transverse charge densities, Phys. Rev. C **82**, 042201 (2010).
[28] Mary Alberg and Gerald A. Miller, Taming the Pion Cloud of the Nucleon, Phys. Rev. Lett. **108**, 172001 (2012).
[29] Chueng-Ryong Ji, W. Melnitchouk, and A. W. Thomas, Equivalence of pion loops in equal-time and light-front dynamics, Phys. Rev. D **80**, 054018 (2009).
[30] M. Burkardt, K. S. Hendricks, Chueng-Ryong Ji, W. Melnitchouk, and A. W. Thomas, Pion momentum distributions in the nucleon in chiral effective theory, Phys. Rev. D **87**, 056009 (2013).
[31] Chueng-Ryong Ji, W. Melnitchouk, and A. W. Thomas, Anatomy of relativistic pion loop corrections to the electromagnetic nucleon coupling, Phys. Rev. D **88**, 076005 (2013).
[32] Yusupujiang Salamu, Chueng-Ryong Ji, W. Melnitchouk, and P. Wang, $\bar{d}-\bar{u}$ Asymmetry in the Proton in Chiral Effective Theory, Phys. Rev. Lett. **114**, 122001 (2015).

[33] C. Granados and C. Weiss, Light-front representation of chiral dynamics in peripheral transverse densities, J. High Energy Phys. 07 (2015) 170.
[34] C. Granados and C. Weiss, Light-front representation of chiral dynamics with Δ isobar and large-N_c relations, J. High Energy Phys. 06 (2016) 075.
[35] G. Peter Lepage and Stanley J. Brodsky, Exclusive processes in perturbative quantum chromodynamics, Phys. Rev. D **22**, 2157 (1980).
[36] Stanley J. Brodsky, Hans-Christian Pauli, and Stephen S. Pinsky, Quantum chromodynamics and other field theories on the light cone, Phys. Rep. **301**, 299 (1998).
[37] Stanley J. Brodsky, Dae Sung Hwang, Bo-Qiang Ma, and Ivan Schmidt, Light cone representation of the spin and orbital angular momentum of relativistic composite systems, Nucl. Phys. **B593**, 311 (2001).
[38] Yuri V. Kovchegov and Eugene Levin, *Quantum Chromodynamics at High Energy* (Cambridge University Press, Cambridge, England, 2012), Vol. 33.
[39] Thomas Becher and H. Leutwyler, Baryon chiral perturbation theory in manifestly Lorentz invariant form, Eur. Phys. J. C **9**, 643 (1999).
[40] V. Pascalutsa, Quantization of an interacting spin—3/2 field and the Delta isobar, Phys. Rev. D **58**, 096002 (1998).
[41] Tung-Mow Yan, Quantum field theories in the infinite momentum frame 3. Quantization of coupled spin one fields, Phys. Rev. D **7**, 1760 (1973).
[42] Gerald A. Miller, Light front treatment of nuclei: Formalism and simple applications, Phys. Rev. C **56**, 2789 (1997).
[43] Anthony William Thomas and Wolfram Weise, *The Structure of the Nucleon* (Wiley, Germany, 2001).
[44] Pierre A. M. Guichon, Gerald A. Miller, and Anthony William Thomas, The axial form-factor of the nucleon and the pion—nucleon vertex function, Phys. Lett. **124B**, 109 (1983).
[45] J. D. Sullivan, One pion exchange and deep inelastic electron—nucleon scattering, Phys. Rev. D **5**, 1732 (1972).
[46] George F. Sterman, *An Introduction to Quantum Field Theory* (Cambridge University Press, Cambridge, England, 1993).
[47] F. Halzen and Alan D. Martin, *Quarks and Leptons: An Introductory Course in Modern Particle Physics* (Wiley, New York, 1984).
[48] Matthias Aicher, Andreas Schafer, and Werner Vogelsang, Soft-Gluon Resummation and the Valence Parton Distribution Function of the Pion, Phys. Rev. Lett. **105**, 252003 (2010).
[49] Ivan Novikov *et al.*, Parton distribution functions of the charged pion within the xFitter framework, Phys. Rev. D **102**, 014040 (2020).
[50] M. Gluck, E. Reya, and I. Schienbein, Pionic parton distributions revisited, Eur. Phys. J. C **10**, 313 (1999).
[51] Valerio Bertone, Stefano Carrazza, and Juan Rojo, APFEL: A PDF evolution library with QED corrections, Comput. Phys. Commun. **185**, 1647 (2014).
[52] Stefano Carrazza, Alfio Ferrara, Daniele Palazzo, and Juan Rojo, APFEL Web: A web-based application for the graphical visualization of parton distribution functions, J. Phys. G **42**, 057001 (2015).
[53] A. Szczurek, V. Uleshchenko, H. Holtmann, and J. Speth, Production of the *W* bosons and *Z* bosons in the nucleon—anti-nucleon collisions and the meson cloud in the nucleon, Nucl. Phys. **A624**, 495 (1997).
[54] M. Botje, QCDNUM: Fast QCD evolution and convolution, Comput. Phys. Commun. **182**, 490 (2011).
[55] R. Navarro Pérez, J. E. Amaro, and E. Ruiz Arriola, Precise determination of charge dependent pion-nucleon-nucleon coupling constants, Phys. Rev. C **95**, 064001 (2017).
[56] Richard J. Hill, Peter Kammel, William J. Marciano, and Alberto Sirlin, Nucleon axial radius and muonic hydrogen—a new analysis and review, Rep. Prog. Phys. **81**, 096301 (2018).
[57] Veronique Bernard, Latifa Elouadrhiri, and Ulf-G. Meissner, Axial structure of the nucleon: Topical review, J. Phys. G **28**, R1 (2002).
[58] Cezary Juszczak, Running NuWro, Acta Phys. Pol. B **40**, 2507 (2009).
[59] Teppei Katori and Marco Martini, Neutrino–nucleus cross sections for oscillation experiments, J. Phys. G **45**, 013001 (2018).
[60] S. X. Nakamura *et al.*, Towards a unified model of neutrino-nucleus reactions for neutrino oscillation experiments, Rep. Prog. Phys. **80**, 056301 (2017).
[61] Aaron S. Meyer, Minerba Betancourt, Richard Gran, and Richard J. Hill, Deuterium target data for precision neutrino-nucleus cross sections, Phys. Rev. D **93**, 113015 (2016).
[62] R. Bockmann, C. Hanhart, O. Krehl, S. Krewald, and J. Speth, The pi N N vertex function in a meson theoretical model, Phys. Rev. C **60**, 055212 (1999).
[63] Torleif Erik Oskar Ericson, B. Loiseau, and Anthony William Thomas, Determination of the pion nucleon coupling constant and scattering lengths, Phys. Rev. C **66**, 014005 (2002).
[64] E. Oset, H. Toki, and W. Weise, Pionic modes of excitation in nuclei, Phys. Rep. **83**, 281 (1982).
[65] J. M. Eisenberg and D. S. Koltun, *Theory of Meson Interactions with Nuclei* (John Wiley and Sons, Inc. New York, New York, 1980), Chap. 2.
[66] J. A. Niskanen, The $\pi N\Delta$ coupling and the $\Delta(1232)$ resonance width, Phys. Lett. **107B**, 344 (1981).
[67] O. Dumbrajs, R. Koch, H. Pilkuhn, G. c. Oades, H. Behrens, J. j. De Swart, and P. Kroll, Compilation of coupling constants and low-energy parameters. 1982 Edition, Nucl. Phys. **B216**, 277 (1983).
[68] D. Siemens, J. Ruiz de Elvira, E. Epelbaum, M. Hoferichter, H. Krebs, B. Kubis, and U. G. Meißner, Reconciling threshold and subthreshold expansions for pion–nucleon scattering, Phys. Lett. B **770**, 27 (2017).
[69] Véronique Bernard, Evgeny Epelbaum, Hermann Krebs, and Ulf-G. Meißner, New insights into the spin structure of the nucleon, Phys. Rev. D **87**, 054032 (2013).
[70] R. Navarro Pérez, J. E. Amaro, and E. Ruiz Arriola, The low-energy structure of the nucleon–nucleon interaction: Statistical versus systematic uncertainties, J. Phys. G **43**, 114001 (2016).
[71] Evgeny Epelbaum, Hans-Werner Hammer, and Ulf-G. Meissner, Modern theory of nuclear forces, Rev. Mod. Phys. **81**, 1773 (2009).
[72] R. F. Alvarez-Estrada and Anthony William Thomas, Further studies of convergence in the cloudy bag model, J. Phys. G **9**, 161 (1983).
[73] R. S. Towell *et al.* (NuSea Collaboration), Improved measurement of the anti-d/anti-u asymmetry in the nucleon sea, Phys. Rev. D **64**, 052002 (2001).